

---

# ElastiFormer: Learned Redundancy Reduction in Transformer via Self-Distillation

---

**Junzhang Liu\***  
Department of Computer Science  
Columbia University

**Tingkai Liu\*,†‡**  
NeuroAI Scholars  
Cold Spring Harbor Laboratory

**Yueyuan Sui**  
Electrical and Computer Engineering  
Northwestern University

**Stephen Xia†**  
Electrical and Computer Engineering  
Northwestern University

## Abstract

We introduce ElastiFormer, a post-training technique that adapts pretrained Transformer models into an elastic counterpart with variable inference time compute. ElastiFormer introduces small routing modules (as low as .00006% additional trainable parameters) to dynamically select subsets of network parameters and input tokens to be processed by each layer of the pretrained network in an input-dependent manner. The routing modules are trained using self-distillation losses to minimize the differences between the output of the pretrained-model and their elastic counterparts. As ElastiFormer makes no assumption regarding the modality of the pretrained Transformer model, it can be readily applied to all modalities covering causal language modeling, image modeling as well as visual-language modeling tasks. We show that 20% to 50% compute saving could be achieved for different components of the transformer layer, which could be further reduced by adding very low rank LoRA weights (rank 1) trained via the same distillation objective. Finally, by comparing routing trained on different subsets of ImageNet, we show that ElastiFormer is robust against the training domain.

## 1 Introduction

The success of Transformer [70] models across various domains has led to increasingly large and computationally intensive architectures. While these models achieve impressive performance, recent works have demonstrated significant redundancies in both the parameters and computations in pretrained large transformer architectures - which can either manifest as unnecessary processing of tokens [7, 56], or activation [16] of model parameters that contribute minimally to the final output.

Several recent studies have attempted to locate these redundancies [16, 12, 53] and to leverage such redundancies via modified/optimized model architectures (e.g. Mixture-of-Depth which skips tokens around transformer layers [57]). However, such approaches often require architectural modifications, extensive retraining or even training from scratch (such as commonly done for sparse Mixture-of-Expert models [22, 34]).

We address these challenges by introducing **ElastiFormer**, a post-training technique that transforms pre-trained Transformer models into elastic alternatives with variable inference time compute. ElastiFormer introduces lightweight routing modules (as little as 0.0006% additional parameters) that dynamically select subsets of network parameters and input tokens to be processed in an

---

\*Equal contributions

†Corresponding: tiliu@cshl.edu, stephen.xia@northwestern.edu

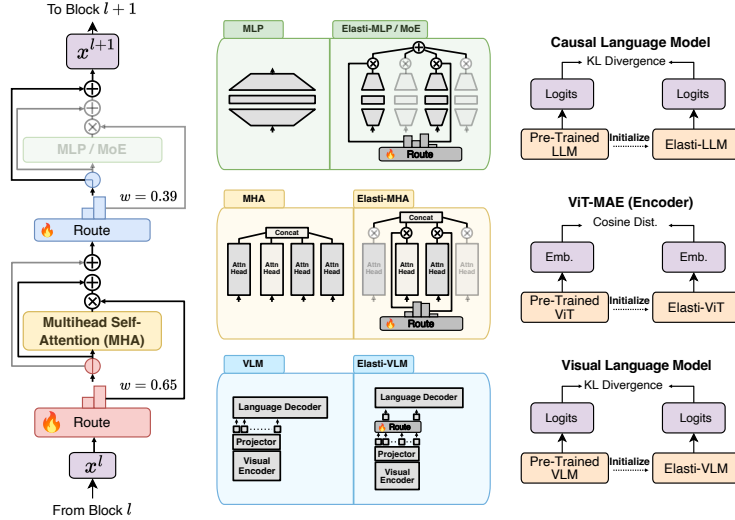


Figure 1: Overview of ElastiFormer for language, visual, and multi-modal transformers. (Left) Illustration of learned routing modules around Multi-Head Attention (MHA) and Multi-layer Perceptron (MLP) modules of a pretrained transformer model. (Middle) Illustration of learned routing modules inside MLP and MHA modules, and learned routing that selects a subset of image tokens that provide multi-modal input to language decoder in VLMs. (Right) Illustration of self-distillation training objectives across modalities. Note that for Visual Transformers (ViT), the example provided here is from Masked Auto Encoding (MAE) ViT.

*input-dependent* manner. These routing modules are trained using self-distillation loss to minimize differences between the output of the pretrained model and their elastic counterparts. Crucially, ElastiFormer makes no assumptions about the modality of the pretrained Transformer model, allowing it to be effectively applied across language, image, and visual-language modalities.

Through extensive experimentation, we demonstrate that 38% (Multi-Head Attention, MHA) and 56% (Multi-Layer Perceptron, MLP) active parameters are required for ElastiFormer to match the performance of the base pretrained model in the language domain. We also show that  $\sim 20\%$  tokens can be dropped from MLP processing (routed to output via residual without going through MLP), while almost all tokens need to be processed by MHA. However, by adding Low-Rank Adaptation (LoRA) weights to MHA with as low as rank 1 learnable parameters, we can drop 20% tokens from MHA processing as well. We observe similar redundancy in parameters and token processing in the visual domain and show that applying ElastiFormer to *even* layers of the pretrained ViT backbone significantly improves performance at equivalent level of compute to applying ElastiFormer to all layers. Applying ElastiFormer to visual-language models, we show that 40% of image tokens can be dropped before being decoded by the language decoder without significantly impacting performance. Finally, by comparing routing modules in Elasti-ViT trained using different subsets of ImageNet, we show that the learned routing is robust to changing data distributions.

In summary, our main contributions are:

1. We introduce ElastiFormer, a post-training technique that converts pretrained transformer models across language, visual, and multi-modal modalities into flexible alternatives with variable inference time compute. ElastiFormer is compatible with other efficient post-training techniques.
2. We demonstrate that with less than 0.3% (as low as 0.00006%) additional learnable parameters, ElastiFormer can reduce the total active parameters or active tokens by 20% to 50% for all modalities without noticeable impact on performance. We also provide extensive analysis of the degree of redundancy in different components of the transformer architecture across modalities.

3. We show that the learned routing is robust to different distributions of training data, thereby providing a reliable representation for interpreting learned representations in pretrained models.

## 2 Related Works

**Efficient Transformer Processing** There is a large body of work aimed at improving transformer efficiency that falls into several categories: mixture of experts (MoE), mixture of depths (MoD), pruning, and quantization [78, 60, 18, 44, 41, 43]. Our work is compatible with existing post-training techniques, such as QLoRA [18], but is most similar in spirit to MoE, MoD, and pruning. Since the introduction of MoE in transformer architectures [61], there have been a flurry of developments, including more efficient MoE architectures [31, 15], sparsification of dense MLPs [85], incorporating gating functions for routing [82, 34], and realizing LLMs at scales larger than ever [22].

Pruning is another class of techniques used to statically remove redundant weights (unstructured) [11, 30] or smaller blocks (structured) in the MHA or FFN layers [47, 21, 37, 2, 76, 77, 9, 80]. Other works focus on pruning or merging context in the KV cache [3, 79] or individual patches in vision transformers [67, 33].

Most similar to our work is the recent development of MoD [57], which proposes learnable routers that “skip” less relevant transformer layers in an input-dependent and compute-adjustable manner. In contrast to “early exit” methods [59, 45], which skip any remaining transformer layers, MoD may skip middle layers and still process later layers. Other works have shown varying levels of spatial and temporal redundancies in transformer architectures [19, 12, 16], and introduce methods for efficiently identifying and removing them during inference (e.g., skipping attention heads [28]). In contrast, our work provides a general learning framework for discovering and bypassing redundancies to enable more efficient processing pathways through pretrained transformer models.

**Knowledge Distillation (KD) and Domain Generalization.** KD is a class of techniques that transfer knowledge from one model to another (often smaller), where the structure of the models are generally fixed [29, 65, 36, 73, 58, 69, 26, 66, 75, 40, 81]. Self-distillation (SD) is a sub-class of KD, where the student and teacher models are the same architecture. In many cases, the SD aims to distill knowledge learned in deeper layers to shallow layers in the same model, which has shown to reduce overfitting, improve domain generalization, and embed semantic information that is not commonly seen in non-SD models [64, 54, 8, 63, 35, 46, 32, 38, 74]. Most of these works focus on pretraining to improve task performance, while we incorporate SD as a mechanism to self learn router weights to reduce computation in an input-dependent and non-sequential manner.

**Mechanistic Interpretability (MI).** MI has recently emerged as a promising class of techniques for interpreting deep neural networks and transformer architectures [51, 55] by decomposing models into smaller components and identifying human interpretable “features” and their pathways that form subnetworks or “circuits”. A key question in MI is to explore the notion of “universality” or how similar features, activations, or circuits arise between different models and tasks. While many works have explored and identified how each component (e.g., MHA and FFN sublayers) functions within transformer architectures [20, 48, 49, 62, 23], there are mixed results when it comes to discovering universality. Several works have identified similar components, such as induction and duplication heads, that develop across different models and tasks [52, 24, 72, 50], while others observe that different weight initializations for the same task result in different circuits and representations [84, 13]. We believe our work could be used to study the interpretability of transformer architectures by analyzing the learned routers across different model architectures and domains.

## 3 Redundancy in Transformer Architecture

We first demonstrate that pretrained transformer models have data-dependent redundancies in both their multi-head attention (MHA) and multi-layer perceptron (MLP) modules. We progressively dropped attention heads and MLP layers in a pretrained Gemma-2-2b-it [68] model, and quantified the performance degradation on both mathematical reasoning (GSM8K[14]) and code generation (HumanEval[10]) tasks. Note that in these experiments, no additional learnable parameters were introduced.

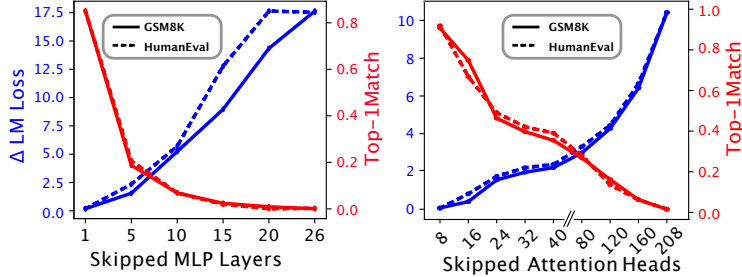


Figure 2: Difference in language modeling loss (blue) and top-1 token prediction agreement (red) between pretrained Gemma2 model and Gemma2 model with skipped MLP layers (left) or attention heads in MHA (right). Experiments are performed for both GSM8K (solid line) and HumanEval (dashed line) datasets.

For each experiment, we randomly select a progressively larger number of attention-heads and MLP layers to remove and calculate the total differences in language modeling losses as well as the percentage agreement of the vocabulary index predicted by the base and pruned model. As illustrated in Figure 2, skipping a small number of heads or layers has negligible impact on model performance, with faster performance deterioration observed when skipping more MLP layers than removing attention heads. Importantly, the performance scaling differ between GSM8K and HumanEval datasets, indicating that the redundancy in the pretrained LLM is data-dependent. These results motivated us to explore learned, data-dependent routing modules that not only skip MLP layers and attention heads in a learnable manner, but also skip attention layers and subsets of MLP weights. As later demonstrated, ElastiFormer offers significantly higher degree of compute savings over static pruning at comparable performance degradation.

## 4 ElastiFormer - Learned Routing of Transformer Models via Self-Distillation

Given the redundancy in pre-trained Transformer models, we seek a lightweight post-training technique to minimize the number of active parameters necessary without significantly deteriorating overall performance. Consequently, we propose ElastiFormer which introduces lightweight learned, input-dependent routing modules that route input tokens (regardless of modality) through a subset of the pre-trained Transformer network.

Depending on the modality, ElastiFormer introduces 4-5 routing modules that control routing around and within all modules of the transformer architecture (i.e. Multi-Head Attention, MLP). The routing schemes can be roughly divided into two categories (see Figure. 3):

- **Input Subset Selection:** For this type of subset selection, given a sequence of  $T$  tokens, we select  $k$  to be processed by a given module (e.g. MHA, MLP). This routing scheme saves computational cost by reducing the total number of *input tokens* processed. Examples of routing in ElastiFormer that employ this scheme are routing around MHA, around MLP (Figure 1(Left)), and visual token selection in VLM (Figure 1(Mid-Bottom)).
- **Parameter Subset Selection:** For this type of subset selection, the total number of inputs to a given module remains unchanged. Instead, we save computational cost by reducing the number of active parameters within a given module that is used to process the given input. Examples of routing in ElastiFormer that employ this scheme are routing within MHA (attention head selection) and within MLP (expert selection).

### 4.1 Parameter Subset Selection

We consider the routing problem where we are given input token  $x_t \in \mathbb{R}^D$ , and  $M$  subsets of sub-networks  $f_1, \dots, f_M$  ( $M \ll D$ ). A simple router (linear projector) is trained to select top  $k$ ,  $1 \leq k \leq M$  sub-networks to process the given input following the procedure outlined in Algorithm 1.

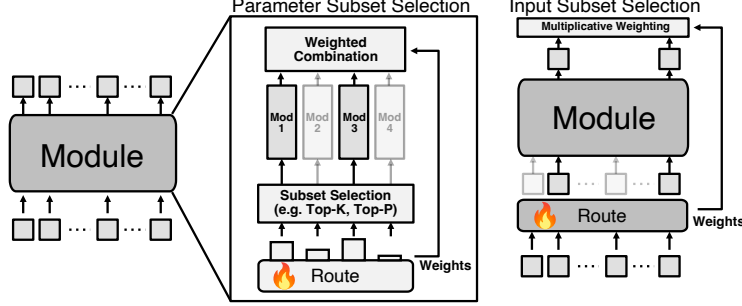


Figure 3: Illustration of the two subset selection schemes employed in the current work. For parameter subset selection, the sub-modules (Mod 1-4) that are selected by the routing scheme can either refer to the attention heads in MHA or experts in MLP. Note that to create experts in MLP from a pretrained dense MLP layer, we first transform the dense MLP parameters to block matrices that form the experts. In either routing scheme, the routing weights are multiplied with the output to ensure gradient flow.

---

**Algorithm 1** Parameter Subset Selection w/ Linear Router

---

**Require:** Input token  $x_t \in \mathbb{R}^D$   
**Require:** Set of sub-networks  $\{f_m\}_{m=1}^M$   
**Require:** Number of routes to select  $k$ , where  $1 \leq k \leq M$   
**Require:** Router parameters  $W_r \in \mathbb{R}^{M \times D}$

- 1:  $w_t \leftarrow M \cdot \text{softmax}(W_r x_t)$  ▷ Routing Weights
- 2:  $\{(m_i, w_{t,m_i})\}_{i=1}^k \leftarrow \text{top-k}(w_t, k)$  ▷ Subset Selection
- 3: **for**  $i = 1$  to  $k$  **do**
- 4:  $y_{t,m_i} \leftarrow w_{t,m_i} \cdot f_{m_i}(x_t)$  ▷ Sub-network Forward
- 5: **end for**

**return**  $y_t = \text{Aggregate}(\{y_{t,m_i}\}_i)$

---

At the high level, the parameter subset selection works essentially the same as the Mixture-of-Expert routing with a straight-through estimator for gradient propagation, with the noticeable difference that the weight vector is normalized to sum to  $M$ . This additional normalization ensures that when the router selects all sub-networks (number of routes  $k = M$ ) with uniform routing weights  $w_{t,i} = 1 \forall i = 1, \dots, k$ , the overall input/output of the routed network is *exactly* the same as the pre-trained model without routing.

The sub-network  $\{f_m\}_m$  could either refer to processing via individual attention heads or via an expert in the Mixture-of-Expert MLP module. As many pre-trained transformer models have dense MLP layers (no experts), ElastiFormer converts a dense MLP module to a MoE counterpart losslessly by breaking parameters into block matrices. Consider a simple MLP with 1 hidden layer, we can rewrite the input/output relationship of the dense MLP as the equivalent MoE MLP with 2-experts:

$$y_t = W_2 \sigma(W_1 x_t) = [W_{2,1} \quad W_{2,2}] \sigma \left( \begin{bmatrix} W_{1,1} \\ W_{1,2} \end{bmatrix} x_t \right),$$

where  $\sigma(\cdot)$  is some element-wise nonlinearity, and  $W_{1,i}, W_{2,i}$  are block matrices obtained by splitting the weight matrices row-wise and column-wise respectively. While we found decomposing the pretrained weights to block matrices sufficient, we acknowledge that alternative initialization of MoE MLP from dense MLP exists and have been explored by contemporary works [85, 82, 86]. We leave further explorations of MoE initialization from dense MLP in the context of ElastiFormer for further work.

**Input Subset Selection** We consider the routing problem where we are given input token  $x_{1:T} \in \mathbb{R}^{T \times D}$  and a given module  $f : \mathbb{R}^D \mapsto \mathbb{R}^D$ . A router is trained to select top  $k, 1 \leq k \leq T$  tokens to process by the module following the Algorithm 2.

As opposed to parameter subset selection where the router outputs a  $M$ -dimensional logits for  $M$  sub-networks, the routers in input subset selection output scalar-valued logits for each input token.

---

**Algorithm 2** Input Subset Selection w/ Linear Router

---

**Require:** Input tokens  $x_{1:T} \in \mathbb{R}^{T \times D}$

**Require:** Module  $f$

**Require:** Number of tokens to select  $k$ , where  $1 \leq k \leq T$

**Require:** Router parameters  $W_r \in \mathbb{R}^D$

1:  $w \leftarrow \text{softmax}(W_r x_{1:T})$

▷ Routing weights  $w \in \mathbb{R}^T$

2:  $I \leftarrow \text{top-k}(w, k)$

▷ Index set of selected input

3:  $y_{1:T} \leftarrow \mathbf{0} \in \mathbb{R}^{T \times D}$

▷ Zero-initialized output

4:  $y_{t \in I} \leftarrow w_{t \in I} \cdot f(x_{t \in I})$

**return**  $y$

---

The top- $k$  input tokens are then processed by the subsequent module (MHA or MLP), and the output is added to a zero-initialized output tensor with the same shape as the un-selected input  $x_{1:T}$ .

Note that, as discussed in [57], for causal language models that generate tokens auto-regressively, the top- $k$  token selection only applies to the training phase and not the inference phase - where causality dictates whether a given token will be in the top- $k$  cannot be determined without first completing the generation of the entire sequence. Authors of [57] proposed two approaches to predict whether a given token will be in the top- $k$  during inference time based on 1) the output logits of the same router that computes the routing weights, or 2) output logits of an additional dedicated classification MLP that similarly maps input embedding  $x_t$  to a scalar logit value. Within the context of ElastiFormer, we found the two methods of top- $k$  prediction during inference to give similar performance and opted to use the former (same router for top- $k$  prediction) to minimize additional learnable parameters.

## 4.2 Objective Function

The primary training objective of ElastiFormer is distillation loss  $\mathcal{L}_{\text{distill}}$ . For causal language modeling and visual-language modeling where the output modality is language, we compute KL-divergence between the student model’s output probability  $p_{\text{student}}$  and the teacher model’s output probability  $p_{\text{teacher}}$ . We compared different modifications of the KL-divergence objective for distillation losses on a toy problem, where the teacher model is a pretrained GPT-Neo-125M [6] model, and the student model is initialized from teacher model with Gaussian parameter noised and a rank-32 LoRA adapter for `q_proj`, `v_proj` components in the MHA module. The student model is trained on the GSM8K training dataset using combinations of three different types of modifications to the KL-divergence objective (see also Figure 4):

- Forward  $D_{KL}(p_{\text{student}}||p_{\text{teacher}})$  versus Reverse KL  $D_{KL}(p_{\text{teacher}}||p_{\text{student}})$  [71, 25]
- Top-K KL [4]: convert the teacher model’s output probability over vocabulary to a  $k + 1$  dimensional vector, where the first  $k$  values correspond to the probability of the top- $k$  tokens in the vocabulary with the highest probability, and the last value is the residual probability to ensure the  $k + 1$  probability vector sums to 1. The student model’s output is arranged using the top- $k$  token indices of the teacher model.
- Temperature scaling [83]: divide the logits of student and teacher model outputs by a positive scalar temperature before converting to probability distribution via softmax.

As shown in Figure 4, the language modeling loss of the student model on the evaluation dataset shows that forward KL loss of top-50 tokens leads to the best performance and fastest convergence rate, which is the distillation loss we adopted in the current work for both language modeling and visual-language modeling tasks. For image modeling (applying ElastiFormer to ViT-MAE [27]), we chose the cosine distance between the student image encoder’s output token embedding and that of the teacher model for simplicity. Note that as the output token embedding of the ViT-encoder is normalized via LayerNorm, minimizing cosine distance is equivalent to maximizing the inner product between student and teacher token embedding.

In addition to the distillation loss, ElastiFormer training involves additional auxiliary losses for the two types of routing modules described above.

For routing modules that perform *parameter* subset selection, the routers are additionally trained using load-balancing loss  $\mathcal{L}_{\text{load}}$  which minimizes the weighted sum of input tokens processed by each

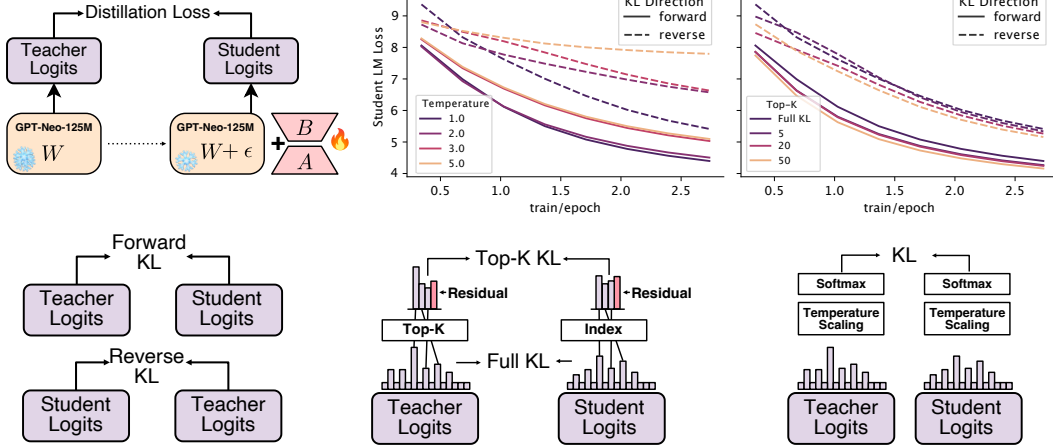


Figure 4: Comparison between different distillation losses for language output modality. The three types of variations of the KL-divergence objectives are illustrated on the bottom row.

sub-network. While such load-balancing loss is crucial for MoE models where both the experts and the routers are trainable to prevent mode collapse and ensure balanced sub-network utilization, its effect is much less pronounced for ElastiFormer where the sub-networks are frozen. Nevertheless, we found this auxiliary loss to be beneficial for stabilizing training of router modules especially for very low  $k$  values (very few sub-networks activated).

For routing modules that perform input subset selection, we only include auxiliary loss in the case of *causal* language modeling. As mentioned in the previous section, during inference, scalar logits of a token selection module are used to determine if a given token will likely be in the top- $k$  of the final generated sequence or not. Consequently, during the training phase, binary cross-entropy loss  $\mathcal{L}_{\text{top-k}}$  between the scalar logits and one-hot encoding of whether the corresponding token is indeed in top- $k$  is introduced as an auxiliary loss to the input subset selection for causal LMs [57].

As such the overall objective for ElastiFormer is:

$$\mathcal{L} = \mathcal{L}_{\text{distill}} + \lambda_{\text{load}} \mathcal{L}_{\text{load}} + \underbrace{\lambda_{\text{top-k}} \mathcal{L}_{\text{top-k}}}_{\text{for Causal LM}} \quad (1)$$

In practice, we found  $\lambda_{\text{load}} = \lambda_{\text{top-k}} = 1$  to be sufficient for convergence of all evaluated model architectures.

## 5 Experiments

In this section, we describe in detail the experimental setup and findings of the current work. For reference, we included the total number of additional parameters introduced for each ElastiFormer experiment in Table 1 which highlights that ElastiFormer introduces *minimal* (0.25% ~ 0.00006%) additional learnable parameters while achieving significant redundancy reduction across modalities. Unless otherwise specified, all experiments were performed on 1 NVIDIA H100 NVL 96GB GPU with AdamW optimization of learning rate  $1e-4$  and cosine learning rate scheduler with 3% warmup.

### 5.1 Elasti-LLM - ElastiFormer for Causal Language Model

**Experimental Setup** We applied ElastiFormer to both Phi-3.5-mini-instruct [1] and Gemma-2-2b-it [68] pretrained language models, where the models were trained via self-distillation on the GSM8K [14] training set (7.5K question/answer pairs) for 3 epochs and batch-size of 32.

**Scaling of Performance vs. Capacity** We begin by performing an extensive ablation study of the 4 types of routing in Elasti-LLM shown in Figure 5.

Selection	Module	# Params.	Elasti-LLM		Elasti-ViT	Elasti-VLM
			Gemma2-2B	Phi3-Mini	ViT-MAE-L	LLaVA-1.5
Input	MLP	$L \times (D + 2)$	60K (.003%)	98K (.003%)	25K (.01%)	-
	MHA	$L \times (D + 2)$	60K (.003%)	98K (.003%)	25K (.01%)	-
	VLM/L	$D + 2$	-	-	-	4K (.00006%)
	VLM/M	$D^2 + 2D + 2$	-	-	-	17M (.23%)
Param.	MLP	$L \times (D \times M)$	2M (.08%)	3M (.08%)	0.8M (.24%)	-
	MHA	$L \times (D \times M)$	2M (.08%)	3M (.08%)	0.8M (.24%)	-

Table 1: Number of trainable parameters introduced by ElastiFormer with percentage of total number of parameters of pre-trained base model shown in parenthesis.  $L$  is the number of layers,  $D$  is the hidden dimension and  $M$  is the number of sub-networks (number of attention heads or number of experts in MoE-MLP). VLM/L, VLM/M refer to linear or MLP routing modules applied to image tokens selection in VLM.

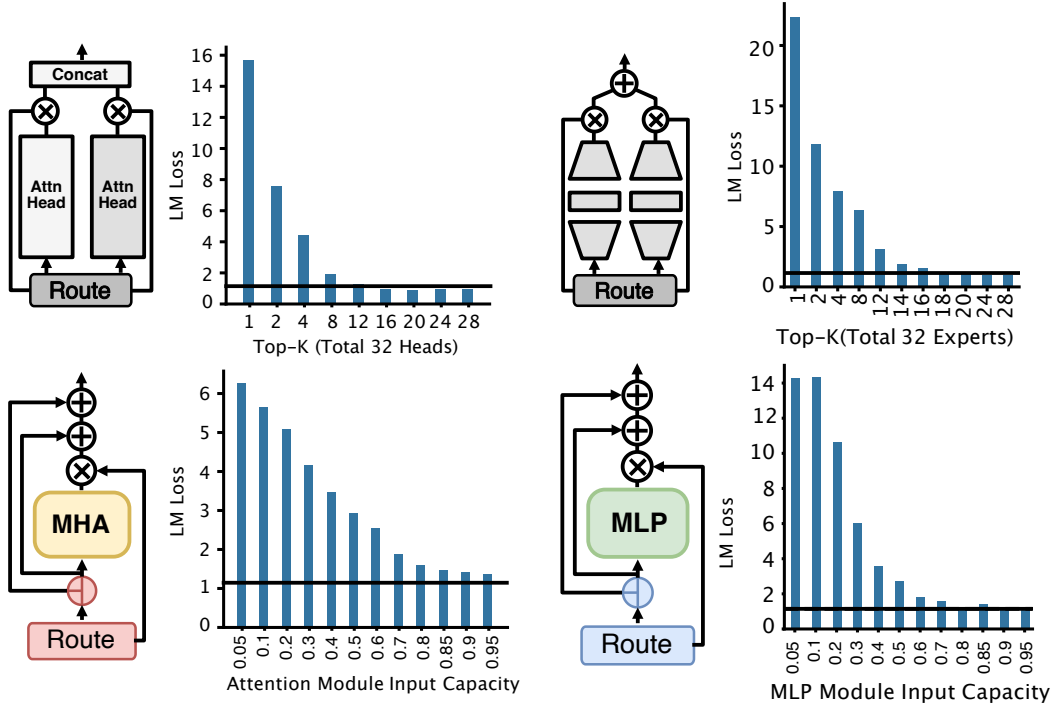


Figure 5: Scaling of various modules in Elasti-LLM against compute for elastic Phi-3.5-mini-instruct. LM Loss of the pretrained teacher model is shown as the horizontal black line in each of the subfigures.

As shown in the figure, we are able to achieve the same level of performance (as measured by LM Loss) as the teacher model with 38% attention heads (12/32), 56% active parameters in MLP (18/32 experts initialized from the pretrained dense MLP module), 80% token processing through the MLP module. We note that deactivating 20/32 attention heads in *each* layer corresponds to a total number of 640 skipped attention heads, which is dramatically higher than the pruning results shown in Figure 2.

In contrast to the above-mentioned 3 routing schemes, input selection for the *attention* module could not reach the base model performance even with high input capacity. This is likely due to the context-dependency of processing in the MHA module, which makes input selection that is only based on single token embedding (without context) challenging. While this result appears contradictory to those reported in MoD [57], we note that a key difference between ElastiFormer and MoD is that modules in ElastiFormer are completely frozen apart from lightweight routing modules. In contrast, the MoD model trains both the model backbone and routing module simultaneously. Motivated by this, we experimented with adding a small amount of learnable parameters to the MHA module to compensate for the deterioration of performance caused by input selection. We added LoRA modules



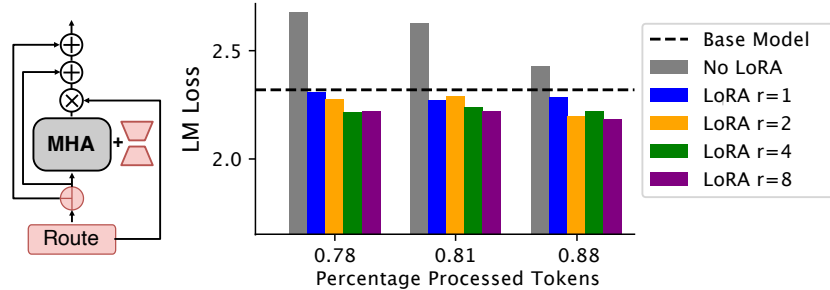


Figure 6: Scaling of Gemma-2-2B-it across a percentage of processed tokens with LoRA adapter for Q, V projections in MHA. The ElastiFormer module is trained with input subset selection for both MHA and MLP modules, as well as parameter subset selection for the MLP module (with 4 experts and top-2 selection).

to the MHA’s  $q\_proj, v\_proj$  weights, which allowed us to achieve the same performance of the teacher model with relatively low lora-rank. The results are shown in Figure 6, which compares the impact of varying LoRA ranks ( $r$ ) for an elastic gemma-2-2b-it model across different capacity levels. Even with rank 1 adapters added to Q, V projections in MHA modules (0.008% trainable parameters), LoRA-enhanced Elasti-LLM achieves performance comparable to the teacher model, with additional trainable weights (higher ranks) leading to even lower loss. Interestingly, we observe that the LM loss of Elasti-LLM can even be lower than that of the base pretrained model, which is consistent with previous literature on self-distillation improving model performance [64, 8].

## 5.2 Elasti-ViT - ElastiFormer for Vision Transformer

**Experimental Setup** We applied ElastiFormer to vit-mae-large [27] pretrained ViT models and trained the *encoder* part of the ViT-MAE model via self-distillation on a 10% subset of the ImageNet-1K [17] training set ( $\sim 1M$  images) for 3 epochs with batch-size of 900. The training objective minimizes the cosine distance between Elasti-ViT’s output token embedding and that of the pretrained ViT-MAE model, while the evaluation is done by comparing the cosine similarities between the *decoder* output between student and teacher models (reconstructed images).

**Scaling of Performance vs. Capacity** Similar to scaling analysis for causal language models, we performed scaling analysis of Elasti-ViT for different level of subset selection of the 4 different types of routing modules. We evaluate the performance of each experiment by cosine similarity between the MAE decoder (pretrained and frozen) outputs when given encoder output of Elasti-ViT encoder and the based encoder. Example reconstructions are shown in the Supplementary Materials.

Contrary to the experiments in language modeling, results in Figure 7 show that only input selection for MLP module is able to achieve  $> 0.95$  cosine similarity with teacher model’s decoder output with input capacity  $> 0.8$  (dropping 20% input tokens to MLP modules). This is potentially caused by the much smaller size of ViT-MAE-L models, which has 330M parameters which less than 10% of the size of Phi-3.5-mini-instruct.

We explore an alternative technique to improve the performance of Elasti-ViT, instead of adding learnable LoRA modules, we applied ElastiFormer to only *even* layers of the ViT-MAE model. Applying ElastiFormer to even layers reduces computational savings by half while simultaneously reducing the learnable routing parameters by half. As shown in Figure 7, when Elasti-ViT with even layer routing significantly improves the model performance, where 50% MHA Attention-Heads, 31% MLP active parameters, 70% active tokens for MHA and 10% active tokens for MLP are sufficient to achieve  $> 0.95$  cosine similarity to the teacher model’s decoder output. More importantly, by preserving computing in half of the layers, we are able to achieve higher saturating performance of Elasti-ViT. Note that this approach to applying ElastiFormer to even layers is also compatible with adding LoRA weights, which could further improve computational savings as in the case for Elasti-LLM.

Additionally, we examined the robustness of learned routing of Elasti-ViT against different distributions of training data. To this end, we trained 10 instances of Elasti-ViT using 10 subsets of ImageNet

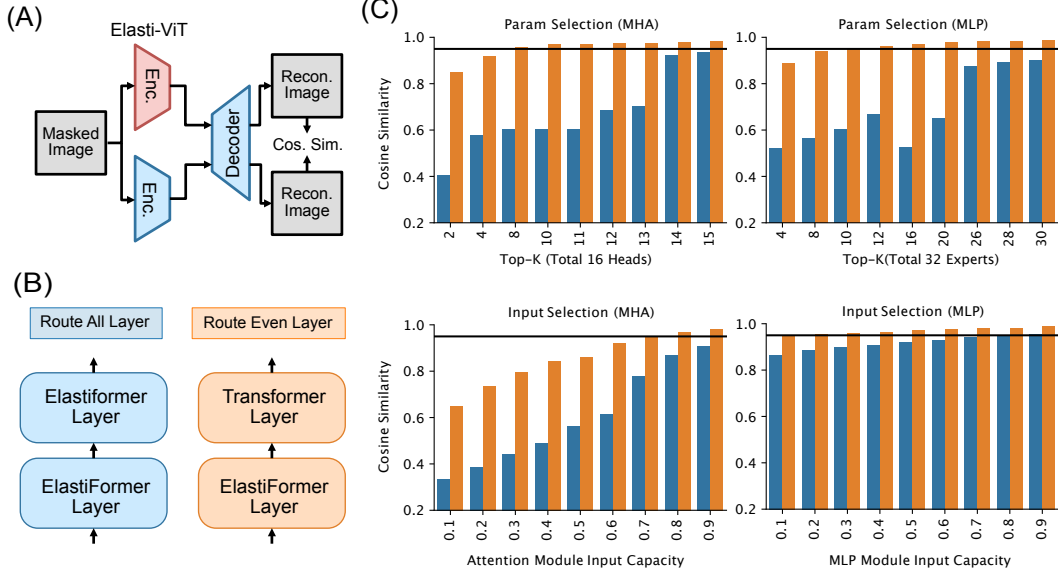


Figure 7: Scaling of Elasti-ViT (ViT-MAE-L) performance on held-out ImageNet-1K test set as measured by cosine similarity between MAE decoder output when given encoder output of Elasti-ViT and base pretrained encoder (as shown in (A)). Experiments are shown for both ViT-MAE with ElastiFormer for all layers or only even layer (as shown in (B)). Horizontal black lines in (C) indicate a cosine similarity of 0.95, which we use as a threshold for when the Elasti-ViT recovers the output of the pretrained ViT-MAE model. Note that as shown in (A), only the encoder has a trainable router in the Elasti-ViT experiments.

based on categories proposed by [39]. We then computed the pairwise cosine similarities between router activations of the 10 Elasti-ViTs instances on held-out evaluation images, as shown by the 10x10 similarity matrix shown in Figure 8(Left). All routers shown high similarities, with routers trained on similar classes (e.g. ape and monkey, aquatic bird and bird) show higher similarities than others. The robustness of the learned routing to training data is further demonstrated in Figure 8 (Right), where similar the patches of the same image are selected by Elasti-ViT routers trained on different image classes.

### 5.3 Elasti-VLM - ElastiFormer for Visual Language Model

**Training and Evaluation Setup** We applied ElastiFormer to llava-v1.5-7b [42] pretrained visual-language models, which the was trained via self-distillation on a 10K subset of the 665K LLaVA-Instruct dataset for 1 epoch with batch-size of 32.

**Scaling of Performance vs. Capacity** Since experiments for causal LMs and ViTs have established results on redundancy in image encoder and language decoder respectively, we focus our experiments on Elasti-VLM to redundancy in image tokens (output of the visual encoder) processed by the language decoder. In particular, we added an input subset selection routing module that selects the top-k image tokens to be processed by the language decoder as shown in Figure 1(Mid-Bottom).

We evaluated Elasti-VLM’s performance on both OpenChair [5] hallucination benchmark and LLava-Bench [42] open domain QA benchmark, and compared against performance of the base pretrained VLM model (llava-v1.5-7b). We additionally experimented with more complex routing modules with an MLP router with 1 hidden layer and GELU activation function. As shown in Figure 9, the LLava-Bench results show that Elasti-VLM is able to achieve the same performance as the base model with 60% 70% of input tokens, and is able to even outperform the base model for complex and conversational tasks. However, for tasks that required detailed visual information such as LLava-Bench (detail) and OpenChair which evaluates VLM’s ability to accurately describe all key objects in an image, Elasti-VLM offers no clear advantage over the base VLM model.

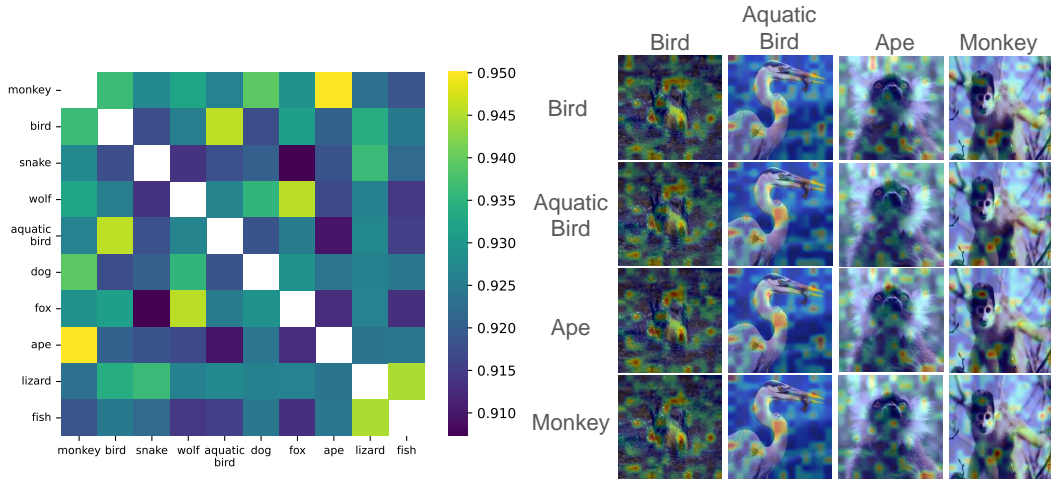


Figure 8: Comparing learned routing of Elasti-ViT trained using different subsets of ImageNet. (Left) Cosine similarities between router logits for ten classes in ImageNet. Labels indicate the class of images that an Elasti-ViT instance is trained on. (Right) Heatmap of patches selected by different instances of Elasti-ViT routers. Each row corresponds to a different Elasti-ViT instance trained on a given image class.

When comparing routing modules of different complexities, results in Figure 9 suggests that the additional parameters in MLP routers is able to improve Elasti-VLM’s performance, albeit at a significant computational cost (0.23% additional routing parameters for MLP router compared to 0.00006% for linear router as shown in Table 1). We leave further explorations of complexity of routing modules to ElastiFormer performance for future research.

## 6 Summary & Discussion

ElastiFormer demonstrates that significant computational savings can be obtained through learned routing across modalities, and can be readily incorporated into existing post-training pipelines with techniques such as LoRA. Our method far out-performs static pruning of model parameters with minimal additional parameters and robust learned routing, which provides practical tools for not only model efficiency but also interpreting learned representations in various components of the transformer architecture.

An interesting finding of the current work, and perhaps a key limitation, is that the computational savings of skipping tokens from processing by attention modules do not perform as well as other sources of computational savings (skipping attention heads, skipping MLP blocks, reducing MLP active parameters). While this performance degradation can be rescued by very low-rank LoRA adapters for the attention module, it raises the question of the type of redundancy that exists in attention computation. We hypothesize that the comparatively poor performance of input subset selection for MHA is due to the design of the routing module, which performs routing based on *individual* token embedded in a way that is agnostic to context. Indeed, choosing the tokens that have the least impact on MHA module output requires knowing *a priori* the degree to which this token will be attended to by other tokens. One potential improvement of the current formulation of ElastiFormer is to compute the routing of tokens for the MHA module based on not only the token embedding but also the attention weights of previous layers. We leave explorations of alternative methods for routing tokens for MHA layer for future works.

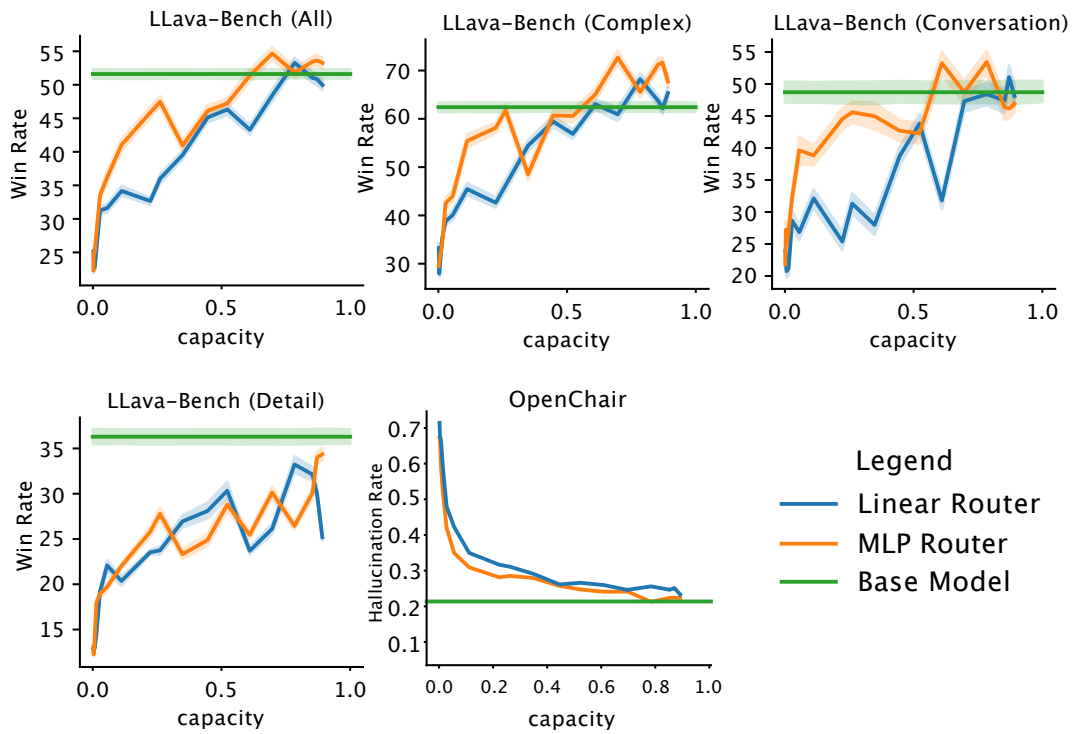


Figure 9: Evaluation of Elasti-LLaVA on LLava-Bench and OpenChair benchmarks against capacity. The capacity value indicates the percentage of image tokens selected by the ElastiFormer routing module. Error bar for LLava-Bench results indicate 95% confidence interval obtained via bootstrap sampling (100 samples with replacement).

## References

- [1] Marah Abdin, Jyoti Aneja, Hany Awadalla, Ahmed Awadallah, Ammar Ahmad Awan, Nguyen Bach, Amit Bahree, Arash Bakhtiari, Jianmin Bao, Harkirat Behl, Alon Benhaim, Misha Bilenko, Johan Bjorck, Sébastien Bubeck, Martin Cai, Qin Cai, Vishrav Chaudhary, Dong Chen, Dongdong Chen, Weizhu Chen, Yen-Chun Chen, Yi-Ling Chen, Hao Cheng, Parul Chopra, Xiyang Dai, Matthew Dixon, Ronen Eldan, Victor Fragoso, Jianfeng Gao, Mei Gao, Min Gao, Amit Garg, Allie Del Giorno, Abhishek Goswami, Suriya Gunasekar, Emman Haider, Junheng Hao, Russell J. Hewett, Wenxiang Hu, Jamie Huynh, Dan Iter, Sam Ade Jacobs, Mojan Javaheripi, Xin Jin, Nikos Karampatziakis, Piero Kauffmann, Mahoud Khademi, Dongwoo Kim, Young Jin Kim, Lev Kurilenko, James R. Lee, Yin Tat Lee, Yuanzhi Li, Yunsheng Li, Chen Liang, Lars Liden, Xihui Lin, Zeqi Lin, Ce Liu, Liyuan Liu, Mengchen Liu, Weishung Liu, Xiaodong Liu, Chong Luo, Piyush Madan, Ali Mahmoudzadeh, David Majercak, Matt Mazzola, Cao César Teodoro Mendes, Arindam Mitra, Hardik Modi, Anh Nguyen, Brandon Norick, Barun Patra, Daniel Perez-Becker, Thomas Portet, Reid Pryzant, Heyang Qin, Marko Radmilac, Liliang Ren, Gustavo de Rosa, Corby Rosset, Sambudha Roy, Olatunji Ruwase, Olli Saarikivi, Amin Saied, Adil Salim, Michael Santacrose, Shital Shah, Ning Shang, Hiteshi Sharma, Yelong Shen, Swadheen Shukla, Xia Song, Masahiro Tanaka, Andrea Tupini, Praneetha Vaddamanu, Chunyu Wang, Guanhua Wang, Lijuan Wang, Shuohang Wang, Xin Wang, Yu Wang, Rachel Ward, Wen Wen, Philipp Witte, Haiping Wu, Xiaoxia Wu, Michael Wyatt, Bin Xiao, Can Xu, Jiahang Xu, Weijian Xu, Jilong Xue, Sonali Yadav, Fan Yang, Jianwei Yang, Yifan Yang, Ziyi Yang, Donghan Yu, Lu Yuan, Chenruidong Zhang, Cyril Zhang, Jianwen Zhang, Li Lyna Zhang, Yi Zhang, Yue Zhang, Yunan Zhang, and Xiren Zhou. Phi-3 technical report: A highly capable language model locally on your phone, 2024.
- [2] Yongqi An, Xu Zhao, Tao Yu, Ming Tang, and Jinqiao Wang. Fluctuation-based adaptive structured pruning for large language models. In *Proceedings of the AAAI Conference on Artificial Intelligence*, volume 38, pages 10865–10873, 2024.
- [3] Sotiris Anagnostidis, Dario Pavllo, Luca Biggio, Lorenzo Noci, Aurelien Lucchi, and Thomas Hofmann. Dynamic context pruning for efficient and interpretable autoregressive transformers. *Advances in Neural Information Processing Systems*, 36, 2024.
- [4] Amanda Askell, Yuntao Bai, Anna Chen, Dawn Drain, Deep Ganguli, Tom Henighan, Andy Jones, Nicholas Joseph, Ben Mann, Nova DasSarma, Nelson Elhage, Zac Hatfield-Dodds, Danny Hernandez, Jackson Kernion, Kamal Ndousse, Catherine Olsson, Dario Amodei, Tom Brown, Jack Clark, Sam McCandlish, Chris Olah, and Jared Kaplan. A general language assistant as a laboratory for alignment, 2021.
- [5] Assaf Ben-Kish, Moran Yanuka, Morris Alper, Raja Giryes, and Hadar Averbuch-Elor. Mitigating open-vocabulary caption hallucinations, 2024.
- [6] Sid Black, Leo Gao, Phil Wang, Connor Leahy, and Stella Biderman. GPT-Neo: Large Scale Autoregressive Language Modeling with Mesh-Tensorflow, March 2021. If you use this software, please cite it using these metadata.
- [7] Daniel Bolya, Cheng-Yang Fu, Xiaoliang Dai, Peizhao Zhang, Christoph Feichtenhofer, and Judy Hoffman. Token merging: Your vit but faster. *arXiv preprint arXiv:2210.09461*, 2022.
- [8] Mathilde Caron, Hugo Touvron, Ishan Misra, Hervé Jégou, Julien Mairal, Piotr Bojanowski, and Armand Joulin. Emerging properties in self-supervised vision transformers. In *Proceedings of the IEEE/CVF international conference on computer vision*, pages 9650–9660, 2021.
- [9] Arnav Chavan, Zhiqiang Shen, Zhuang Liu, Zechun Liu, Kwang-Ting Cheng, and Eric P Xing. Vision transformer slimming: Multi-dimension searching in continuous optimization space. In *Proceedings of the IEEE/CVF Conference on Computer Vision and Pattern Recognition*, pages 4931–4941, 2022.
- [10] Mark Chen, Jerry Tworek, Heewoo Jun, Qiming Yuan, Henrique Ponde de Oliveira Pinto, Jared Kaplan, Harri Edwards, Yuri Burda, Nicholas Joseph, Greg Brockman, Alex Ray, Raul Puri, Gretchen Krueger, Michael Petrov, Heidy Khlaaf, Girish Sastry, Pamela Mishkin, Brooke Chan, Scott Gray, Nick Ryder, Mikhail Pavlov, Alethea Power, Lukasz Kaiser, Mohammad Bavarian, Clemens Winter, Philippe Tillet, Felipe Petroski Such, Dave Cummings, Matthias Plappert, Fotios Chantzis, Elizabeth Barnes, Ariel Herbert-Voss, William Hebgen Guss, Alex Nichol, Alex Paino, Nikolas Tezak, Jie Tang, Igor Babuschkin, Suchir Balaji, Shantanu Jain,

- William Saunders, Christopher Hesse, Andrew N. Carr, Jan Leike, Josh Achiam, Vedant Misra, Evan Morikawa, Alec Radford, Matthew Knight, Miles Brundage, Mira Murati, Katie Mayer, Peter Welinder, Bob McGrew, Dario Amodei, Sam McCandlish, Ilya Sutskever, and Wojciech Zaremba. Evaluating large language models trained on code. 2021.
- [11] Tianlong Chen, Jonathan Frankle, Shiyu Chang, Sijia Liu, Yang Zhang, Zhangyang Wang, and Michael Carbin. The lottery ticket hypothesis for pre-trained bert networks. *Advances in neural information processing systems*, 33:15834–15846, 2020.
  - [12] Tianlong Chen, Zhenyu Zhang, Yu Cheng, Ahmed Awadallah, and Zhangyang Wang. The principle of diversity: Training stronger vision transformers calls for reducing all levels of redundancy. In *Proceedings of the IEEE/CVF Conference on Computer Vision and Pattern Recognition*, pages 12020–12030, 2022.
  - [13] Bilal Chughtai, Lawrence Chan, and Neel Nanda. A toy model of universality: Reverse engineering how networks learn group operations. In *International Conference on Machine Learning*, pages 6243–6267. PMLR, 2023.
  - [14] Karl Cobbe, Vineet Kosaraju, Mohammad Bavarian, Mark Chen, Heewoo Jun, Lukasz Kaiser, Matthias Plappert, Jerry Tworek, Jacob Hilton, Reiichiro Nakano, Christopher Hesse, and John Schulman. Training verifiers to solve math word problems. *arXiv preprint arXiv:2110.14168*, 2021.
  - [15] Damai Dai, Chengqi Deng, Chenggang Zhao, RX Xu, Huazuo Gao, Deli Chen, Jiashi Li, Wangding Zeng, Xingkai Yu, Y Wu, et al. Deepseekmoe: Towards ultimate expert specialization in mixture-of-experts language models. *arXiv preprint arXiv:2401.06066*, 2024.
  - [16] Fahim Dalvi, Hassan Sajjad, Nadir Durrani, and Yonatan Belinkov. Analyzing redundancy in pretrained transformer models. *arXiv preprint arXiv:2004.04010*, 2020.
  - [17] Jia Deng, Wei Dong, Richard Socher, Li-Jia Li, Kai Li, and Li Fei-Fei. Imagenet: A large-scale hierarchical image database. In *2009 IEEE Conference on Computer Vision and Pattern Recognition*, pages 248–255, 2009.
  - [18] Tim Dettmers, Artidoro Pagnoni, Ari Holtzman, and Luke Zettlemoyer. Qlora: Efficient finetuning of quantized llms. *Advances in Neural Information Processing Systems*, 36, 2024.
  - [19] Matthew Dutson, Yin Li, and Mohit Gupta. Eventful transformers: leveraging temporal redundancy in vision transformers. In *Proceedings of the IEEE/CVF International Conference on Computer Vision*, pages 16911–16923, 2023.
  - [20] Nelson Elhage, Neel Nanda, Catherine Olsson, Tom Henighan, Nicholas Joseph, Ben Mann, Amanda Askell, Yuntao Bai, Anna Chen, Tom Conerly, et al. A mathematical framework for transformer circuits. *Transformer Circuits Thread*, 1(1):12, 2021.
  - [21] Gongfan Fang, Xinyin Ma, Mingli Song, Michael Bi Mi, and Xinchao Wang. Depgraph: Towards any structural pruning. In *Proceedings of the IEEE/CVF conference on computer vision and pattern recognition*, pages 16091–16101, 2023.
  - [22] William Fedus, Barret Zoph, and Noam Shazeer. Switch transformers: Scaling to trillion parameter models with simple and efficient sparsity, 2022.
  - [23] Mor Geva, Roei Schuster, Jonathan Berant, and Omer Levy. Transformer feed-forward layers are key-value memories. *arXiv preprint arXiv:2012.14913*, 2020.
  - [24] Rhys Gould, Euan Ong, George Ogden, and Arthur Conmy. Successor heads: Recurring, interpretable attention heads in the wild. *arXiv preprint arXiv:2312.09230*, 2023.
  - [25] Yuxian Gu, Li Dong, Furu Wei, and Minlie Huang. MiniLLM: Knowledge distillation of large language models. In *The Twelfth International Conference on Learning Representations*, 2024.
  - [26] Zhiwei Hao, Jianyuan Guo, Ding Jia, Kai Han, Yehui Tang, Chao Zhang, Han Hu, and Yunhe Wang. Learning efficient vision transformers via fine-grained manifold distillation. *Advances in Neural Information Processing Systems*, 35:9164–9175, 2022.
  - [27] Kaiming He, Xinlei Chen, Saining Xie, Yanghao Li, Piotr Dollár, and Ross Girshick. Masked autoencoders are scalable vision learners, 2021.
  - [28] Shwai He, Guoheng Sun, Zheyu Shen, and Ang Li. What matters in transformers? not all attention is needed. *arXiv preprint arXiv:2406.15786*, 2024.

- [29] Geoffrey Hinton. Distilling the knowledge in a neural network. *arXiv preprint arXiv:1503.02531*, 2015.
- [30] Shaoyi Huang, Dongkuan Xu, Ian EH Yen, Yijue Wang, Sung-En Chang, Bingbing Li, Shiyang Chen, Mimi Xie, Sanguthevar Rajasekaran, Hang Liu, et al. Sparse progressive distillation: Resolving overfitting under pretrain-and-finetune paradigm. *arXiv preprint arXiv:2110.08190*, 2021.
- [31] Gagan Jain, Nidhi Hegde, Aditya Kusupati, Arsha Nagrani, Shyamal Buch, Prateek Jain, Anurag Arnab, and Sujoy Paul. Mixture of nested experts: Adaptive processing of visual tokens. *arXiv preprint arXiv:2407.19985*, 2024.
- [32] Ye-Rin Jeoung, Jeong-Hwan Choi, Ju-Seok Seong, JeHyun Kyung, and Joon-Hyuk Chang. Self-distillation into self-attention heads for improving transformer-based end-to-end neural speaker diarization. In *Proceedings of the Annual Conference of the International Speech Communication Association, INTERSPEECH*, volume 2023, pages 3197–3201. International Speech Communication Association, 2023.
- [33] Yiren Jian, Tingkai Liu, Yunzhe Tao, Chunhui Zhang, Soroush Vosoughi, and Hongxia Yang. Expedited training of visual conditioned language generation via redundancy reduction. In *Proceedings of the 62nd Annual Meeting of the Association for Computational Linguistics (Volume 1: Long Papers)*, pages 300–314, 2024.
- [34] Albert Q Jiang, Alexandre Sablayrolles, Antoine Roux, Arthur Mensch, Blanche Savary, Chris Bamford, Devendra Singh Chaplot, Diego de las Casas, Emma Bou Hanna, Florian Bressand, et al. Mixtral of experts. *arXiv preprint arXiv:2401.04088*, 2024.
- [35] Jue Jiang, Neelam Tyagi, Kathryn Tringale, Christopher Crane, and Harini Veeraraghavan. Self-supervised 3d anatomy segmentation using self-distilled masked image transformer (smit). In *International Conference on Medical Image Computing and Computer-Assisted Intervention*, pages 556–566. Springer, 2022.
- [36] Xiaoqi Jiao, Yichun Yin, Lifeng Shang, Xin Jiang, Xiao Chen, Linlin Li, Fang Wang, and Qun Liu. Tinybert: Distilling bert for natural language understanding. *arXiv preprint arXiv:1909.10351*, 2019.
- [37] Bo-Kyeong Kim, Geonmin Kim, Tae-Ho Kim, Thibault Castells, Shinkook Choi, Junho Shin, and Hyoung-Kyu Song. Shortened llama: A simple depth pruning for large language models. *arXiv preprint arXiv:2402.02834*, 11, 2024.
- [38] Seanie Lee, Minki Kang, Juho Lee, Sung Ju Hwang, and Kenji Kawaguchi. Self-distillation for further pre-training of transformers. *arXiv preprint arXiv:2210.02871*, 2022.
- [39] Youngsoo Lee and Seongjoo Moon. Clustered imagenet labels for training production-friendly image classifier. <https://github.com/Prev/clustered-imagenet-labels>, 2021.
- [40] Sihao Lin, Hongwei Xie, Bing Wang, Kaicheng Yu, Xiaojun Chang, Xiaodan Liang, and Gang Wang. Knowledge distillation via the target-aware transformer. In *Proceedings of the IEEE/CVF Conference on Computer Vision and Pattern Recognition*, pages 10915–10924, 2022.
- [41] Yang Lin, Tianyu Zhang, Peiqin Sun, Zheng Li, and Shuchang Zhou. Fq-vit: Post-training quantization for fully quantized vision transformer. *arXiv preprint arXiv:2111.13824*, 2021.
- [42] Haotian Liu, Chunyuan Li, Qingyang Wu, and Yong Jae Lee. Visual instruction tuning. In *Thirty-seventh Conference on Neural Information Processing Systems*, 2023.
- [43] Shih-Yang Liu, Zechun Liu, and Kwang-Ting Cheng. Oscillation-free quantization for low-bit vision transformers. In *International Conference on Machine Learning*, pages 21813–21824. PMLR, 2023.
- [44] Zhenhua Liu, Yunhe Wang, Kai Han, Wei Zhang, Siwei Ma, and Wen Gao. Post-training quantization for vision transformer. *Advances in Neural Information Processing Systems*, 34:28092–28103, 2021.
- [45] Zhuang Liu, Zhiqiu Xu, Hung-Ju Wang, Trevor Darrell, and Evan Shelhamer. Anytime dense prediction with confidence adaptivity. *arXiv preprint arXiv:2104.00749*, 2021.
- [46] Hui Ma, Jian Wang, Hongfei Lin, Bo Zhang, Yijia Zhang, and Bo Xu. A transformer-based model with self-distillation for multimodal emotion recognition in conversations. *IEEE Transactions on Multimedia*, 2023.

- [47] Xinyin Ma, Gongfan Fang, and Xinchao Wang. Llm-pruner: On the structural pruning of large language models. *Advances in neural information processing systems*, 36:21702–21720, 2023.
- [48] Callum McDougall, Arthur Conmy, Cody Rushing, Thomas McGrath, and Neel Nanda. Copy suppression: Comprehensively understanding an attention head. *arXiv preprint arXiv:2310.04625*, 2023.
- [49] Kevin Meng, David Bau, Alex Andonian, and Yonatan Belinkov. Locating and editing factual associations in gpt. *Advances in Neural Information Processing Systems*, 35:17359–17372, 2022.
- [50] Jack Merullo, Carsten Eickhoff, and Ellie Pavlick. Circuit component reuse across tasks in transformer language models. *arXiv preprint arXiv:2310.08744*, 2023.
- [51] Chris Olah, Nick Cammarata, Ludwig Schubert, Gabriel Goh, Michael Petrov, and Shan Carter. Zoom in: An introduction to circuits. *Distill*, 5(3):e00024–001, 2020.
- [52] Catherine Olsson, Nelson Elhage, Neel Nanda, Nicholas Joseph, Nova DasSarma, Tom Henighan, Ben Mann, Amanda Askell, Yuntao Bai, Anna Chen, et al. In-context learning and induction heads. *arXiv preprint arXiv:2209.11895*, 2022.
- [53] Bowen Pan, Rameswar Panda, Yifan Jiang, Zhangyang Wang, Rogerio Feris, and Aude Oliva. Ia-red 2: Interpretability-aware redundancy reduction for vision transformers. *Advances in Neural Information Processing Systems*, 34:24898–24911, 2021.
- [54] Sangjoon Park, Gwanghyun Kim, Yujin Oh, Joon Beom Seo, Sang Min Lee, Jin Hwan Kim, Sungjun Moon, Jae-Kwang Lim, Chang Min Park, and Jong Chul Ye. Self-evolving vision transformer for chest x-ray diagnosis through knowledge distillation. *Nature communications*, 13(1):3848, 2022.
- [55] Daking Rai, Yilun Zhou, Shi Feng, Abulhair Saparov, and Ziyu Yao. A practical review of mechanistic interpretability for transformer-based language models. *arXiv preprint arXiv:2407.02646*, 2024.
- [56] Yongming Rao, Wenliang Zhao, Benlin Liu, Jiwen Lu, Jie Zhou, and Cho-Jui Hsieh. Dynamicvit: Efficient vision transformers with dynamic token sparsification. *Advances in neural information processing systems*, 34:13937–13949, 2021.
- [57] David Raposo, Sam Ritter, Blake Richards, Timothy Lillicrap, Peter Conway Humphreys, and Adam Santoro. Mixture-of-depths: Dynamically allocating compute in transformer-based language models. *arXiv preprint arXiv:2404.02258*, 2024.
- [58] Victor Sanh, L Debut, J Chaumond, and T Wolf. Distilbert, a distilled version of bert: Smaller, faster, cheaper and lighter. *arXiv preprint arXiv:1910.01108*, 2019.
- [59] Tal Schuster, Adam Fisch, Jai Gupta, Mostafa Dehghani, Dara Bahri, Vinh Tran, Yi Tay, and Donald Metzler. Confident adaptive language modeling. *Advances in Neural Information Processing Systems*, 35:17456–17472, 2022.
- [60] Wenqi Shao, Mengzhao Chen, Zhaoyang Zhang, Peng Xu, Lirui Zhao, Zhiqian Li, Kaipeng Zhang, Peng Gao, Yu Qiao, and Ping Luo. Omniquant: Omnidirectionally calibrated quantization for large language models. *arXiv preprint arXiv:2308.13137*, 2023.
- [61] Noam Shazeer, Azalia Mirhoseini, Krzysztof Maziarz, Andy Davis, Quoc Le, Geoffrey Hinton, and Jeff Dean. Outrageously large neural networks: The sparsely-gated mixture-of-experts layer. *arXiv preprint arXiv:1701.06538*, 2017.
- [62] Alessandro Stolfo, Yonatan Belinkov, and Mrinmaya Sachan. A mechanistic interpretation of arithmetic reasoning in language models using causal mediation analysis. *arXiv preprint arXiv:2305.15054*, 2023.
- [63] Sungho Suh, Vitor Fortes Rey, and Paul Lukowicz. Tasked: transformer-based adversarial learning for human activity recognition using wearable sensors via self-knowledge distillation. *Knowledge-Based Systems*, 260:110143, 2023.
- [64] Maryam Sultana, Muzammal Naseer, Muhammad Haris Khan, Salman Khan, and Fahad Shahbaz Khan. Self-distilled vision transformer for domain generalization. In *Proceedings of the Asian Conference on Computer Vision*, pages 3068–3085, 2022.
- [65] Siqi Sun, Yu Cheng, Zhe Gan, and Jingjing Liu. Patient knowledge distillation for bert model compression. *arXiv preprint arXiv:1908.09355*, 2019.



- [66] Zhiqing Sun, Hongkun Yu, Xiaodan Song, Renjie Liu, Yiming Yang, and Denny Zhou. Mobilebert: a compact task-agnostic bert for resource-limited devices. *arXiv preprint arXiv:2004.02984*, 2020.
- [67] Yehui Tang, Kai Han, Yunhe Wang, Chang Xu, Jianyuan Guo, Chao Xu, and Dacheng Tao. Patch slimming for efficient vision transformers. In *Proceedings of the IEEE/CVF Conference on Computer Vision and Pattern Recognition*, pages 12165–12174, 2022.
- [68] Gemma Team, Morgane Riviere, Shreya Pathak, Pier Giuseppe Sessa, Cassidy Hardin, Surya Bhupatiraju, Léonard Hussenot, Thomas Mesnard, Bobak Shahriari, Alexandre Ramé, Johan Ferret, Peter Liu, Pouya Tafti, Abe Friesen, Michelle Casbon, Sabela Ramos, Ravin Kumar, Charline Le Lan, Sammy Jerome, Anton Tsitsulin, Nino Vieillard, Piotr Stanczyk, Sertan Girgin, Nikola Momchev, Matt Hoffman, Shantanu Thakoor, Jean-Bastien Grill, Behnam Neyshabur, Olivier Bachem, Alanna Walton, Aliaksei Severyn, Alicia Parrish, Aliya Ahmad, Allen Hutchison, Alvin Abdagic, Amanda Carl, Amy Shen, Andy Brock, Andy Coenen, Anthony Laforge, Antonia Paterson, Ben Bastian, Bilal Piot, Bo Wu, Brandon Royal, Charlie Chen, Chintu Kumar, Chris Perry, Chris Welty, Christopher A. Choquette-Choo, Danila Sinopalnikov, David Weinberger, Dimple Vijaykumar, Dominika Rogozińska, Dustin Herbison, Elisa Bandy, Emma Wang, Eric Noland, Erica Moreira, Evan Senter, Evgenii Eltyshev, Francesco Visin, Gabriel Rasskin, Gary Wei, Glenn Cameron, Gus Martins, Hadi Hashemi, Hanna Klimczak-Plucińska, Harleen Batra, Harsh Dhand, Ivan Nardini, Jacinda Mein, Jack Zhou, James Svensson, Jeff Stanway, Jetha Chan, Jin Peng Zhou, Joana Carrasqueira, Joana Iljazi, Jocelyn Becker, Joe Fernandez, Joost van Amersfoort, Josh Gordon, Josh Lipschultz, Josh Newlan, Ju yeong Ji, Kareem Mohamed, Kartikeya Badola, Kat Black, Katie Millican, Keelin McDonell, Kelvin Nguyen, Kiranbir Sodhia, Kish Greene, Lars Lowe Sjoesund, Lauren Usui, Laurent Sifre, Lena Heuermann, Leticia Lago, Lilly McNealus, Livio Baldini Soares, Logan Kilpatrick, Lucas Dixon, Luciano Martins, Machel Reid, Manvinder Singh, Mark Iverson, Martin Görner, Mat Velloso, Mateo Wirth, Matt Davidow, Matt Miller, Matthew Rahtz, Matthew Watson, Meg Risdal, Mehran Kazemi, Michael Moynihan, Ming Zhang, Minsuk Kahng, Minwoo Park, Mofi Rahman, Mohit Khatwani, Natalie Dao, Nenshad Bardoliwalla, Nesh Devanathan, Neta Dumai, Nilay Chauhan, Oscar Wahltinez, Pankil Botarda, Parker Barnes, Paul Barham, Paul Michel, Pengchong Jin, Petko Georgiev, Phil Culliton, Pradeep Kuppala, Ramona Comanescu, Ramona Merhej, Reena Jana, Reza Ardeshtir Rokni, Rishabh Agarwal, Ryan Mullins, Samaneh Saadat, Sara Mc Carthy, Sarah Cogan, Sarah Perrin, Sébastien M. R. Arnold, Sebastian Krause, Shengyang Dai, Shruti Garg, Shruti Sheth, Sue Ronstrom, Susan Chan, Timothy Jordan, Ting Yu, Tom Eccles, Tom Hennigan, Tomas Kocisky, Tulsee Doshi, Vihan Jain, Vikas Yadav, Vilobh Meshram, Vishal Dharmadhikari, Warren Barkley, Wei Wei, Wenming Ye, Woohyun Han, Woosuk Kwon, Xiang Xu, Zhe Shen, Zhitao Gong, Zichuan Wei, Victor Cotruta, Phoebe Kirk, Anand Rao, Minh Giang, Ludovic Peran, Tris Warkentin, Eli Collins, Joelle Barral, Zoubin Ghahramani, Raia Hadsell, D. Sculley, Jeanine Banks, Anca Dragan, Slav Petrov, Oriol Vinyals, Jeff Dean, Demis Hassabis, Koray Kavukcuoglu, Clement Farabet, Elena Buchatskaya, Sebastian Borgeaud, Noah Fiedel, Armand Joulin, Kathleen Kenealy, Robert Dadashi, and Alek Andreev. Gemma 2: Improving open language models at a practical size, 2024.
- [69] Hugo Touvron, Matthieu Cord, Matthijs Douze, Francisco Massa, Alexandre Sablayrolles, and Hervé Jégou. Training data-efficient image transformers & distillation through attention. In *International conference on machine learning*, pages 10347–10357. PMLR, 2021.
- [70] Ashish Vaswani, Noam Shazeer, Niki Parmar, Jakob Uszkoreit, Llion Jones, Aidan N Gomez, Łukasz Kaiser, and Illia Polosukhin. Attention is all you need. In I. Guyon, U. Von Luxburg, S. Bengio, H. Wallach, R. Fergus, S. Vishwanathan, and R. Garnett, editors, *Advances in Neural Information Processing Systems*, volume 30. Curran Associates, Inc., 2017.
- [71] Bichen Wang, Yuzhe Zi, Yixin Sun, Yanyan Zhao, and Bing Qin. Rkld: Reverse kl-divergence-based knowledge distillation for unlearning personal information in large language models, 2024.
- [72] Kevin Wang, Alexandre Variengien, Arthur Conmy, Buck Shlegeris, and Jacob Steinhardt. Interpretability in the wild: a circuit for indirect object identification in gpt-2 small. *arXiv preprint arXiv:2211.00593*, 2022.
- [73] Wenhui Wang, Furu Wei, Li Dong, Hangbo Bao, Nan Yang, and Ming Zhou. Minilm: Deep self-attention distillation for task-agnostic compression of pre-trained transformers. *Advances in Neural Information Processing Systems*, 33:5776–5788, 2020.

- [74] Xuying Wang, Jiawei Zhu, Zhengliang Yan, Zhaoyang Zhang, Yunsheng Zhang, Yansheng Chen, and Haifeng Li. Last: Label-free self-distillation contrastive learning with transformer architecture for remote sensing image scene classification. *IEEE Geoscience and Remote Sensing Letters*, 19:1–5, 2022.
- [75] Kan Wu, Jinnian Zhang, Houwen Peng, Mengchen Liu, Bin Xiao, Jianlong Fu, and Lu Yuan. Tinyvit: Fast pretraining distillation for small vision transformers. In *European conference on computer vision*, pages 68–85. Springer, 2022.
- [76] Mengzhou Xia, Tianyu Gao, Zhiyuan Zeng, and Danqi Chen. Sheared llama: Accelerating language model pre-training via structured pruning. *arXiv preprint arXiv:2310.06694*, 2023.
- [77] Mengzhou Xia, Zexuan Zhong, and Danqi Chen. Structured pruning learns compact and accurate models. *arXiv preprint arXiv:2204.00408*, 2022.
- [78] Guangxuan Xiao, Ji Lin, Mickael Seznec, Hao Wu, Julien Demouth, and Song Han. Smoothquant: Accurate and efficient post-training quantization for large language models. In *International Conference on Machine Learning*, pages 38087–38099. PMLR, 2023.
- [79] Yuhui Xu, Zhanming Jie, Hanze Dong, Lei Wang, Xudong Lu, Aojun Zhou, Amrita Saha, Caiming Xiong, and Doyen Sahoo. Think: Thinner key cache by query-driven pruning. *arXiv preprint arXiv:2407.21018*, 2024.
- [80] Lu Yu and Wei Xiang. X-pruner: explainable pruning for vision transformers. In *Proceedings of the IEEE/CVF conference on computer vision and pattern recognition*, pages 24355–24363, 2023.
- [81] Shixing Yu, Tianlong Chen, Jiayi Shen, Huan Yuan, Jianchao Tan, Sen Yang, Ji Liu, and Zhangyang Wang. Unified visual transformer compression. *arXiv preprint arXiv:2203.08243*, 2022.
- [82] Zhengyan Zhang, Yankai Lin, Zhiyuan Liu, Peng Li, Maosong Sun, and Jie Zhou. Moefication: Transformer feed-forward layers are mixtures of experts. *arXiv preprint arXiv:2110.01786*, 2021.
- [83] Kaixiang Zheng and EN-HUI YANG. Knowledge distillation based on transformed teacher matching. In *The Twelfth International Conference on Learning Representations*, 2024.
- [84] Ziqian Zhong, Ziming Liu, Max Tegmark, and Jacob Andreas. The clock and the pizza: Two stories in mechanistic explanation of neural networks. *Advances in Neural Information Processing Systems*, 36, 2024.
- [85] Tong Zhu, Xiaoye Qu, Daize Dong, Jiacheng Ruan, Jingqi Tong, Conghui He, and Yu Cheng. Llama-moe: Building mixture-of-experts from llama with continual pre-training. *arXiv preprint arXiv:2406.16554*, 2024.
- [86] Simiao Zuo, Qingru Zhang, Chen Liang, Pengcheng He, Tuo Zhao, and Weizhu Chen. Moebert: from bert to mixture-of-experts via importance-guided adaptation. *arXiv preprint arXiv:2204.07675*, 2022.

## A Pruning Experiments for Analyzing Redundancy in Pretrained LLMs

Here we describe the procedure in which the redundancy in pretrained LLMs is studied as reported in Section 3.

### A.1 Model and Setup

We utilized the **Gemma-2-2b-it** model as the base pretrained LLM for our experiments. The redundancy was analyzed by systematically removing components of the model and evaluating the resulting impact on its performance. Specifically, we focused on two key architectural components:

- **Entire Transformer Layers:** Skipping entire layers in the Transformer architecture.
- **Multi-Head Attention (MHA):** Removing individual attention heads within the Transformer layers.

### A.2 Component Removal Procedure

#### Random Selection:

- We progressively skipped a random subset of full Transformer layers or removed a random subset of attention heads within the MHA module. Random selection ensured that the skipping process did not introduce systematic bias.
- For each target number of components to remove (e.g., 3 Transformer layers or 3 attention heads), we randomly selected 5 distinct groups of components and performed removal separately. The final results for each configuration were obtained by averaging the performance metrics across these 5 groups.
- The number of skipped Transformer layers or removed attention heads was increased incrementally in each experimental configuration to evaluate performance degradation at different levels of model pruning.

#### No Additional Training:

- After skipping Transformer layers or removing attention heads, no additional learnable parameters were introduced. The remaining model weights were frozen, with no fine-tuning or retraining performed.

### A.3 Evaluation Metrics

The impact of skipping Transformer layers or removing attention heads was quantified using the following metrics:

- **Language Modeling Loss Difference ( $\Delta$  LM Loss):** The difference in LM loss between the base model and the modified (pruned) model was computed as:

$$\Delta \text{LM Loss} = \text{Loss}_{\text{pruned}} - \text{Loss}_{\text{original}}$$

This metric captures the overall degradation in predictive performance due to skipping layers or components.

- **Top-1 Token Prediction Agreement (Top-1 Match):** The percentage of tokens for which the pruned model and the base model predicted the same vocabulary index. This is calculated as:

$$\text{Top-1 Match} = \frac{\text{Count}_{\text{matched}}}{\text{Total}_{\text{tokens}}}$$

where  $\text{Count}_{\text{matched}}$  is the number of tokens with identical predictions, and  $\text{Total}_{\text{tokens}}$  is the total number of tokens in the evaluation dataset.

#### A.4 Experimental Tasks and Datasets

The experiments were conducted on two datasets with distinct characteristics:

- **GSM8K:** A benchmark for mathematical reasoning tasks.
- **HumanEval:** A benchmark for code generation tasks.

#### A.5 Results Analysis

The results, visualized in Figure 2 of the main text, reveal the following:

- Skipping a small number of Transformer layers or attention heads caused minimal performance degradation across both datasets.
- **Skipping Transformer Layers:** Performance degradation was more severe as the number of skipped layers increased, with a sharp rise in LM loss and a significant reduction in Top-1 Match.
- **Removing Attention Heads:** The model exhibited greater tolerance to the removal of individual attention heads, with slower performance degradation compared to skipping entire Transformer layers.
- The differing rates of performance degradation between GSM8K and HumanEval suggest that redundancy is task-dependent.

## B Implementation Details of ElastiFormer

ElastiFormer lowers model redundancy through two key mechanisms: input selection and parameter selection. Input selection determines which tokens (inputs) are processed by the transformer layer and which are skipped. Once a token passes through the input selection stage and enters the layer, parameter selection identifies the specific parameters to be utilized during computation. In this section, we will discuss the implementation of each mechanism in detail.

### B.1 Input Subset Selection

**Routing Module** Given a set of tokens  $X = \{x_1, x_2, \dots, x_T\} \in \mathbb{R}^D$  as input to a block  $B : \mathbb{R}^D \rightarrow \mathbb{R}^D$ , the routing module  $R : \mathbb{R}^D \rightarrow [0, 1]$  produces a set of routing scores  $R(T) = \{s_1, s_2, \dots, s_T\}$  which serve as the basis for token selection. The output of block  $B$  with router  $R$  is given by:

$$B_R(X) = \{B(x_t) \cdot \mathbb{1}[R(x_t) > \theta] + x_t | x_t \in X\}$$

Where  $\mathbb{1} : \mathbb{R} \rightarrow \{0, 1\}$  is an indicator function that returns 1 if  $R(x_t) > \theta$  and 0 otherwise. The parameter  $\theta$  acts as the decision threshold for input selection.

The threshold for selection is decided by the capacity factor  $c$ , a hyperparameter. We select tokens with top  $k$  router scores during training, with  $k = c \cdot T$ . However, this is not feasible during inference for causal models: due to the auto-regressive nature of causal language models, the distribution of the routing weights can change during the generation process, and thus the top  $k$  tokens as well, therefore we use a decision threshold of 0.5 during inference instead.

The selection threshold  $\theta$  is determined by a hyperparameter called the capacity factor,  $c$ . During training, tokens are selected based on the top  $k$  routing scores, where  $k = c \cdot T$ . However, this approach is impractical during inference. Due to the auto-regressive nature of language models, the distribution of routing weights can vary throughout the generation process. Consequently, the set of top  $k$  tokens may also change dynamically, making static selection infeasible. Therefore we, use a decision threshold of 0.5 during inference instead.

**Auxiliary Loss** During inference, the router does not enforce the capacity constraint used in training, as it relies on top  $k$  selection. This discrepancy can lead to the router selecting significantly more tokens than intended, as the gradient produced by (B.2) may encourage such behavior. To ensure consistent behavior during inference, we introduce an auxiliary loss to train the router to select a number of tokens close to the capacity factor. The auxiliary loss is defined as:

$$\mathcal{L}_{\text{top-k}} = -(y \log(R(X)) + (1 - y) \log(1 - R(X)))$$

Here,  $y$  is a binary sequence of length  $T$ , with  $c \cdot T$  entries set to 1 (being positives) and  $(1 - c) \cdot T$  of the entries set to 0 (negatives). The positively selected tokens correspond to those that are selected in the selection step and processed by  $B$ . This approach trains the router to maintain a selection count close to the capacity factor even during the inferencing stage.

## B.2 Parameter Subset Selection

**Routing Module** Redundancy in transformer models can arise not only from input tokens but also from the model’s parameters. To address this, we eliminate parameter redundancy by focusing on attention heads and MLP experts. Similar to input selection, for a block  $B$ , we define a router  $R : \mathbb{R}^n \rightarrow [0, 1]^M$  where  $M$  is the number of experts (i.e., individual attention heads or subdivisions of the MLP block). The router selects the top  $k$  experts with the highest routing scores, where  $k$  is a hyperparameter. Unselected experts simply pass their input through without modification, while the selected experts process their input as usual.

**Auxiliary Loss** The selection of experts can be influenced by the initialization of the routing module. Poor initialization may lead to certain experts being persistently selected while others remain idle, irrespective of the input. To mitigate this, we apply a load-balancing loss as described in section 4.2:

$$\mathcal{L}_{\text{load}} = \sum_{m=1}^M \text{count}(\{m|m \in \text{top-k}(R(X))\}) \cdot R(X)_m$$

Here  $\text{count}(\{m|m \in \text{top-k}(R(X))\})$  calculates how often expert  $m$  appears in the top-k selection by the router  $R$ . This loss penalizes experts with higher top-k counts by lowering their routing probabilities while boosting the probabilities of less frequently selected experts. As a result, it ensures more balanced expert utilization and prevents certain experts from remaining idle.

## C ElastiFormer Model Output Examples

### C.1 Elasti-LLM

In figure Figure 10, we provide example outputs of pretrained Gemma-2-2b-it and its elastic counterpart with input subset selection for both MLP/MHA modules with a capacity factor of 0.75 and parameter subset selection for MLP module with capacity 8 (half of the experts).

<p><b>Question:</b> The rug is 5 feet wider than the chair. The couch is 2 feet longer than twice the width of the rug. If the chair is 3 feet wide. How many feet long is the couch?</p> <p style="text-align: center;"><b>Gemma-2-2b-it:</b></p> <p>Note: The rug is 5 feet wider than the chair. The couch is 2 feet longer than twice the width of the rug. If the chair is 3 feet wide. How many feet long is the couch? Here's how to solve it step-by-step: 1. **Find the width of the rug:** The chair is 3 feet wide, and the rug is 5 feet wider, so the rug is 3 + 5 = 8 feet wide. 2. **Find the length of the couch:** The couch is 2 feet longer than twice the width of the rug, so the length of the couch is 8 * 2 + 2 = 18 feet long. **Answer:** The couch is 18 feet long.</p>	<p><b>In/select MLP: 0.75</b> <b>In/select MHA: 0.75</b> <b>MLP Top-K:8</b></p> <p>Here's how to solve the problem: **1. The chair is 3 feet The rug is 5 feet wider than the chair. ** **2. The couch is 2 feet longer than twice the rug. ** **3. Find the width of the rug: The rug is 3 + 5 = 8 feet. ** **4. Find the width of the couch: The couch is 8 * 2 + 2 = 18 feet long. ** The couch is 18 feet long.</p>
--	---

Figure 10: Example output of Gemma-2-2b-it. The capacity of input selection for MLP/MHA and parameter selection are listed above the outputs. The output quality, despite being influenced by the MLP and MHA capacity, still returns the correct answer and reasoning steps.

### C.2 Elasti-ViT

We provide in Figure 11 examples of reconstruction from the Elasti-ViT model across capacities. Each subfigure of the Elasti-ViT reconstruction is labeled by the cosine similarity between the decoder output of Elasti-ViT and the decoder output of the pretrained ViT-MAE model.

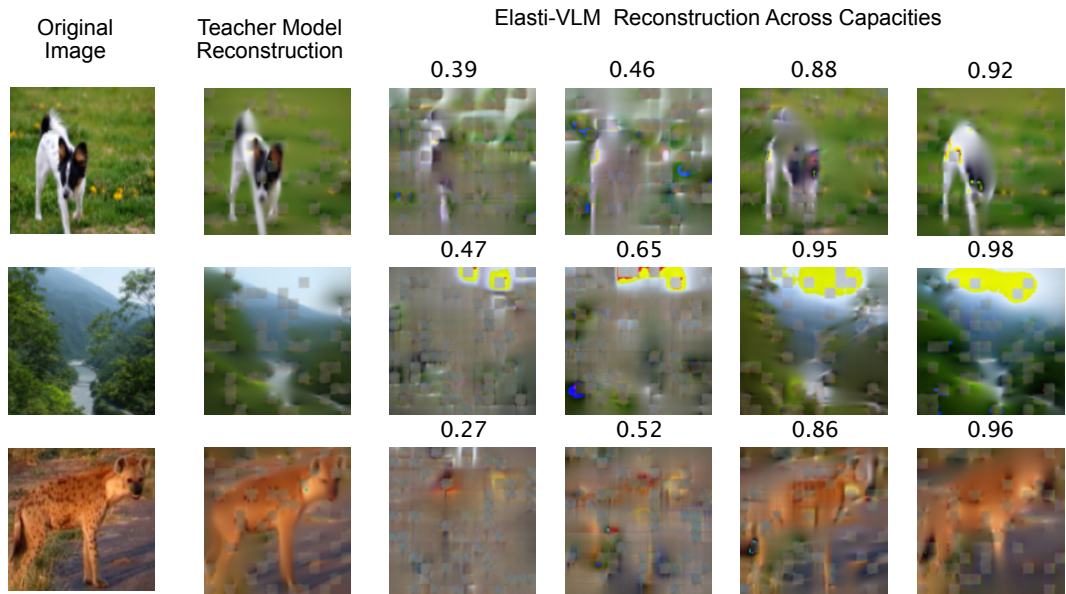
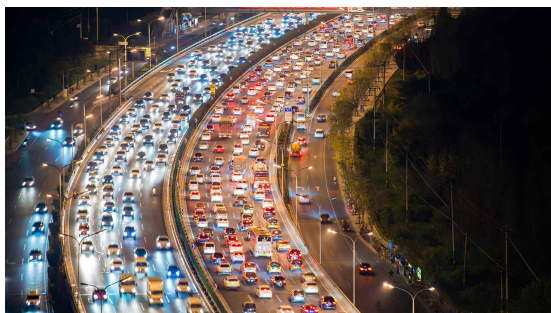


Figure 11: Example reconstruction (decoder output) of ImageNet images from pretrained ViT-MAE and Elasti-ViT with different capacity factors. Each ELasti-ViT subfigure is labeled with cosine similarity against the pretrained ViT-MAE’s decoder output.

### C.3 Elasti-VLM

We provide example outputs of pretrained LLaVA-1.5-7B and its elastic counterpart as shown in Figure 12. According to LLaVA-Bench evaluation script, the scores were computed as the ratio between the score of the Elasti-VLM response and that of the GPT-4 response. The scores were given by llama-3.1-70b-instruct with temperature 0 using the same instruction templates as LLaVA-Bench.



GPT-4

The city might be facing traffic congestion issues, particularly in the four-lane sections of the highway since most cars have their brake lights on, indicating slow or stopped traffic. Possible solutions could include:

1. Implementing traffic management strategies, such as ramp meters to control the rate at which cars enter the highway or optimizing traffic signal timings to improve traffic flow.
2. Encouraging the use of public

.....

Elasti-VLM Linear

Top-2 Token  
Score =0.25

The image shows a city with a large number of people standing in the rain, waiting at a bus stop. This could indicate that the city is facing issues related to public transportation, such as overcrowding, inadequate infrastructure, or inefficient scheduling.

One possible solution to this problem is to invest in improving the public transportation system. This could include expanding the number of buses on the roads, increasing the frequency of buses, or adding more bus

.....

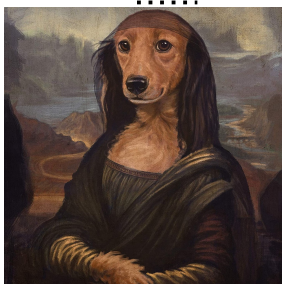
Top-32 Token  
Score =1.12

The city in the image is facing a problem of traffic congestion, as evidenced by the numerous cars on the road and the traffic lights. This can lead to increased travel times, air pollution, and a lower quality of life for the city's residents.

Some possible solutions to this problem include:

1. Implementing public transportation: Encouraging the use of public transportation,

.....



GPT-4

This creative twist on the classic Mona Lisa painting, featuring a dog dressed as the iconic figure, can be interpreted differently by various audiences. Art enthusiasts may view this as an interesting fusion of popular culture and classical art, appreciating the creativity and humor behind the concept. Animal lovers, on the other hand, might be delighted to see a dog take center stage in such a famous piece of art, showcasing the artist's love and appreciation for animals.

For those with a fondness for satire, the image can be seen as poking fun at the seriousness often associated with classical

Elasti-VLM Linear

Top-4 Token  
Score =0.25

The image of a snowman with a Banksy-style head, which combines the innocence and playfulness of a traditional snowman with the rebellious and thought-provoking nature of Banksy's street art, might be interpreted differently by various audiences.

For some, the snowman may evoke a sense of nostalgia and childhood memories, as it is a classic symbol of winter and playtime. The addition of the Banksy-style head could be seen as a commentary on the commercialization and sanitization of childhood, or as a critique of the art world's obsession with fame and fortune.

On the other hand, those who are familiar with Banksy's work may see the snowman as a playful and subversive take on the artist's own style. The juxtaposition of the

Top-350 Token  
Score =1.12

The creative twist on a classic work of art, where a dog is depicted wearing a Renaissance-style dress and a hat, can be interpreted differently by various audiences. Some might find it amusing and lighthearted, as it is an unusual and unexpected sight, while others might perceive it as a commentary on the human tendency to anthropomorphize animals or to assign human-like qualities to non-human beings.

For some, the image could be seen as a playful representation of the bond between humans and their pets, emphasizing the love and care that people often have for their animals. On the other hand, it could also be interpreted as a critique of societal

Figure 12: Example responses of LLava-Bench comparing GPT-4 response and Elasti-VLM response for different top-k image tokens. Errors made by Elasti-VLM are highlighted in red, which led to the low score (score=1 means Elasti-VLM performs as well as GPT-4).